InAsSbBi alloys grown by organometallic vapor-phase epitaxy

K. T. Huang, C. T. Chiu, R. M. Cohen, and G. B. Stringfellow
Department of Materials Science and Engineering, University of Utah, Salt Lake City, Utah 84112

(Received 24 May 1993; accepted for publication 29 November 1993)

A major remaining challenge for III/V semiconductor materials is the development of materials for photonic devices operating in the infrared region of the spectrum. Atmospheric transmission windows exist in the wavelength ranges from 2 to 4.5 and from 8.5 to 12 μm. Thus, emitters and, particularly, detectors operating in these wavelength ranges are important for many applications. Materials for devices operating in the longer-wavelength 8–12 μm region have typically not been III/V semiconductors because the lowest-band-gap conventional III/V alloy is InAsSb, with a 77 K band gap of 0.145 eV, corresponding to a wavelength of 8.5 μm. Previous work has shown that the addition of Bi to InAsSb alloys grown by organometallic vapor-phase epitaxy results in a rapid reduction in the band-gap energy. However, very low temperatures were required to obtained significant levels of Bi incorporation into the solid, due to the immiscibility of Bi in InAsSb. The low growth temperatures result in high carbon contamination levels using conventional precursors. Clearly, new precursors are required for low-temperature growth of these alloys without excessive levels of carbon contamination. New results for the organometallic vapor-phase-epitaxy growth of $InAs_{1-x-y}Sb_xBi_y$ alloys are presented using the novel precursors tertiarybutylarsine, tertiarybutyldimethyl-antimony, and ethyldimethylindium. Alloys have been studied over the entire range of Sb/As ratios in the solid. For growth at 350 °C, the maximum Bi concentration yielding layers without the presence of a liquid second phase was found to be highest for $x=0$ ($y=0.045$) and lowest for $x=0.7$ ($y=0.015$). These levels of Bi incorporation yield calculated 77 K band gaps of 0.08 eV for the alloy with $x=0.5$ and $y=0.015$. These layers have several orders of magnitude lower levels of carbon contamination than reported previously.

I. INTRODUCTION

Infrared (IR) detectors in the wavelength range from 8 to 12 μm are important for a number of military and commercial applications. Several materials systems have been investigated for such applications. The current leading materials are HgCdTe and other II/VI alloys. The extensive research conducted on these materials has clearly shown that while they can be used for detectors over the entire 8–12 μm wavelength range, they are also very difficult to work with, especially the materials for detectors operating beyond 10 μm. Epitaxial growth and other processing steps are much more difficult in these II/VI alloys than for the more highly developed III/V materials. For operation at 12 μm the shift of band gap with composition is large, requiring exquisitely fine control and uniformity of solid composition for fabrication of detector arrays.

The problems are expected to be generally less severe for III/V alloys, since epitaxial growth and processing have become highly developed for other, large-scale applications. For example, several laboratories have succeeded in producing 128×128 element InSb arrays operating at wavelengths out to 7 μm using fairly standard, mature III/V processing.

One reason for the major effort on the II/VI alloys is the inability of conventional III/V alloys to reach 12 μm at the common operating temperature of 77 K. The minimum band gap occurs for $InAs_{0.35}Sb_{0.65}$ at 0.145 eV, or approximately 8.5 μm (Ref. 1) at 77 K.

Several novel structures have been proposed to increase the wavelength range to 12 μm for III/V semiconductors. The concept of using absorption due to transitions between subbands in the quantized conduction-band states of a quantum well or superlattice, primarily in the GaAs/AlGaAs system, has been high touted recently;[2] however, this approach has several disadvantages. Perhaps the major disadvantage is the inability to respond to light striking the detector at normal incidence. A second possible disadvantage is the expected difficulty of obtaining high yield for a process where many superlattice layers are required to be grown with nearly perfect thickness uniformity over large areas for the fabrication of focal plane arrays with the required uniformity of responsivity at a given wavelength. It must be borne in mind that the total active layer thicknesses required for efficient absorption of photons in this region of the spectrum are typically several microns. This makes any superlattice approach possibly even more expensive and difficult to control than the use of HgCdTe. More controversial are suggestions[3] that the ultimate performance of detectors based on this phenomenon will yield values of detectivity significantly lower than for comparable HgCdTe devices. Other suggested superlattice approaches that allow response to normal incidence photons[4] will have the same problems with precise control of the very thick superlattice structures over large lateral dimensions.

Another apparently attractive approach is to use the biaxial tensile strain caused by the lattice mismatch between InAsSb epitaxial layers and the InSb substrate to

 0021-8979/94/75(6)/2857/7/$6.00

reduce the band gap of the InAsSb, or the use of InSb/InAsSb strain layer superlattices.[5] However, the tensile stress in the InAsSb layers produces cracks, which make the material useless for infrared detectors.[6] This will be even more of a problem for the growth of the structures with thicknesses of approximately 10 μm required for high-sensitivity infrared detectors in the 8–12 μm wavelength range.

Our approach is to add Bi to InSb, InAs, and InAsSb alloys. This will produce thick epitaxial layers of a III/V alloy for which existing, well-developed processing technology can be used for IR detector fabrication. Since Bi is much larger than Sb, it produces a rapid reduction in the band gap of InSb of 36 meV/% Bi.[7] We obtain an even larger reduction in band gap for InAs at a rate of 55 meV/% Bi based on both absorption and photoluminescence measurements.[8] Thus, only a few percent of Bi is required for the desired reduction in band-gap energy. This new material is not without its own difficulties. The major problem is with the epitaxial growth. The large size of Bi limits its solubility to approximately 2% (Ref. 9) in InSb, which does not allow operation at 12 μm at 77 K. The solubility limit is even smaller, 0.025%, in InAs.[9]

This lack of solubility of Bi in III/V semiconductor compounds has retarded the development of Bi-containing alloys. Jean-Louis and Hamon[7] were the first to demonstrate the growth of InSbBi alloys. Using relatively high-temperature bulk growth techniques they obtained Bi concentrations of approximately 2%.

In 1980, Zilko and Greene[10] demonstrated that growth at low temperatures using rf sputtering techniques, where the surface atoms have more than thermal energy, allowed the incorporation of much larger amounts of Bi, up to 12% in InSb at a growth temperature of 165 °C. However, the material produced by this technique is of poor quality relative to that produced by epitaxial techniques. Thus, this material could not be used for photonic devices.

Norieka *et al.*[11] used molecular-beam epitaxy (MBE) to grow InSbBi alloys. They reported "Bi concentrations" as high as 2.9% for growth under In-rich conditions. They found the presence of a Bi-rich liquid phase on the surface for growth temperatures above 280 °C. They also discovered that the Bi was incorporated into the InSb films in a form which did not reduce the band gap when Sb-rich growth conditions were used. This suggests that the Bi was not incorporated into the lattice.

Humphreys *et al.*[12] claimed that they had produced InSbBi films with Bi concentrations of 14% by organometallic vapor-phase epitaxy (OMVPE) growth at 445 °C. However, they demonstrated neither a reduction in band gap nor an increase in lattice constant. Only electron microprobe measurements were used to determine the Bi content of the alloy. Unfortunately, this technique averages the composition of any liquid surface phase or other second phase with the composition of the solid. Thus, it is extremely doubtful that the 14% reflects the true, substitutional Bi content of the semiconductor.

Ma *et al.*[8,9] were the first to demonstrate the substitutional incorporation of significant amounts of Bi into InAs and InAsSb alloys. OMVPE growth at low temperatures and V/III ratios of near unity, using the precursors trimethylantimony (TMSb), trimethylindium (TMIn), trimethylbismuth (TMBi), and arsine, was found to result in significant Bi incorporation into the lattice, as evidenced by the resultant increase in the lattice constant, at a rate consistent with the covalent tetrahedral radius of Bi, and a decrease in the band-gap energy. The high quality of these layers is evidenced by the production of photoluminescence (PL) emission, a minority carrier process. However, the InAsBi layers were contaminated with carbon, a donor in these materials, to levels exceeding 10^{19} cm^{-3} at a growth temperature of 300 °C. This is a significant problem for IR detector applications.

Clearly, new precursors are required for the growth of device-quality InAsSbBi layers for operation at wavelengths of 12 μm. TMSb pyrolyzes very slowly at temperatures below 450 °C.[13] The problem is even more severe for arsine.[14] This results in very low utilization efficiencies for this expensive organometallic source. Similarly, the slow pyrolysis rate of TMIn at these low temperatures results in a temperature-dependent growth rate.[15] The temperature-dependent pyrolysis rates of the various precursors results in extreme thickness and compositional nonuniformities associated with temperature gradients in the reactor. Furthermore, the three methyl radicals on the Sb and In precursors apparently give rise to the extremely high carbon contamination levels measured in the InAsSb epitaxial layers.

This article presents new results for the OMVPE growth of $InAs_{1-x}Sb_xBi_y$ alloys using the novel precursors tertiarybutylarsine (TBAs),[14] tertiarybutyldimethyl antimony (TBDMSb),[16] and ethyldimethylindium (EDMIn).[15] These precursors pyrolyze at much lower temperatures than the TMIn, TMSb, and AsH_3 used previously. Alloys have been studied over the entire range of x, from InAs to InSb, at a growth temperature of 350 °C. This approach has given $InAs_{1-x-y}Sb_xBi_y$ alloys with calculated 77 K band gaps of 0.08 eV for the alloy with $x=0.5$ and $y=0.015$. These layers have carbon contamination levels of approximately 3×10^{17} cm^{-3}.

II. EXPERIMENT

An atmospheric pressure, horizontal, infrared-heated OMVPE reactor, with a rectangular cross section 2×5 cm^2 was used for this study. The group-III element, EDMIn, and the group-V elements, TBAs, TBDMSb, and TMBi, enter the reactor through two separate tubes. The precursor bubblers were held in constant temperature baths, with EDMIn at 18 °C, TBDMSb at 23 °C, and both TBAs and TMBi at −20 °C. Pd-diffused hydrogen was used as the carrier gas and the total flow rate was 1.5 ℓ/min. The epitaxial layers were grown at a temperature of 350 °C on various substrates: undoped InAs oriented 2° off (100) toward {100}, exactly (100) InSb, and semi-insulating GaAs oriented 2° off (100) toward {110}.

Before growth the substrates were first degreased in trichloroethane, acetone, and methanol. Then InAs and InSb were etched in 1:1 HF:H_2O for 4 min followed by

TABLE I. Parameters for the OMVPE growth of $InSb_{1-x}Bi_x$ on InSb substrates.

Sample No.	Composition x_{Bi} (at. %)	Thickness (μm)	Temperature T_g (°C)	Molar flow rate (μmol/min)				Input V/III ratio
				EDMIn	TBDMSb	TMBi	Bi/V×100	
ISB 1	1.1	1.00	350	1.131	32.202	0.158	0.488	28.50
ISB 3	1.9	0.80	350	1.131	32.500	0.263	0.803	28.81

0.5% Br in methanol for 2 min. The GaAs was etched in H_2SO_4 for 3 min followed by 1:1:4 H_2O:H_2O_2:H_2SO_4 for 4 min. After rinsing in de-ionized water the substrates were blown dry with nitrogen and immediately transferred into the reactor chamber.

The surface morphologies of the epilayers were observed using Nomarski differential interference contrast microscopy. Layer thicknesses, typically 1–2 μm, were determined by observing the heteroepitaxial interface between the epilayer and substrate on a cleaved cross section. The typical growth rate was 0.65 μm/h. The growth efficiency (epilayer thickness in μm per mole of group-III precursor) is higher using EDMIn than using TMIn at these low substrate temperatures, as reported previously.[9]

The crystallinity and lattice constant were determined using a DIANO XRD-800 x-ray diffractometer. The solid composition of $InAs_{1-x}Sb_x$ samples was determined from x-ray diffraction assuming Vegard's law, but the solid composition for $InAs_{1-x-y}Sb_xBi_y$ could not be determined from the lattice constant. Thus, a Cameca SX-50 electron microprobe was used for the determination of composition of these layers. Standard corrections were used.

Some epilayers, grown on semi-insulating GaAs substrates, were characterized by Hall-effect measurements using the Van der Pauw technique. The In contacts on the four corners of the rectangular samples were annealed at 300 °C for 3 min under a N_2 ambient. The magnetic field was 5 kG and the sample current was between 0.1 and 1 mA, depending on the carrier concentration. An Ar-ion laser operating at either 4480 or 5145 Å was used to excite photoluminescence (PL) for epilayers held at 10 K. The PL was collected by paraboloidal mirrors and focused onto the entrance slit of a Spex monochromator with an InSb or HgCdTe detector positioned near the exit slit.

III. RESULTS AND DISCUSSION

Both InSbBi and InAsSbBi alloys have been grown in this study. The results are presented separately below.

A. InSbBi growth

Previous studies[8] showed that incorporation of Bi without formation of a second phase is more difficult for InSb than for InAs. Table I lists the parameters used for the InSbBi growth runs on InSb substrates. The highest Bi concentration that could be produced without formation of a second phase on the surface is only approximately 2%. The growth of layers with even this small Bi content is difficult. The range of V/III ratio giving smooth surface morphologies is extremely narrow. For V/III ratios slightly higher than optimum, Sb hillocks are formed on the surface. The narrow range of V/III ratio yielding acceptable morphologies is due to the low volatility of metallic Sb at 350 °C. A wider range of V/III ratio can be used for InAsBi alloys. V/III ratios slightly lower than optimum give rise to In droplets that produce whisker growth by the vapor-liquid-solid (VLS) mechanism.

Figure 1 shows x-ray diffraction scans along with morphologies for layers grown using the conditions listed in Table I. The x-ray scans clearly distinguished the $K_{\alpha 1}$ and $K_{\alpha 2}$ x-ray lines. This demonstrates high crystalline quality for these layers. 77 K Hall-effect measurements, performed on layers grown on semi-insulating GaAs substrates, indicate that the addition of few percent Bi has little effect on the background electron concentration, with InSb layers having $n=1.8\times10^{17}$ cm^{-3} and $InSb_{0.981}Bi_{0.019}$ having $n=2.2\times10^{17}$ cm^{-3}. This indicates that TMBi is a reasonable Bi precursor, at these Bi concentrations, in spite of the three methyl radicals per molecule.

B. InAsSbBi growth

The growth of InSbBi alloys is limited to small Bi concentrations, insufficient to reduce the band-gap energy

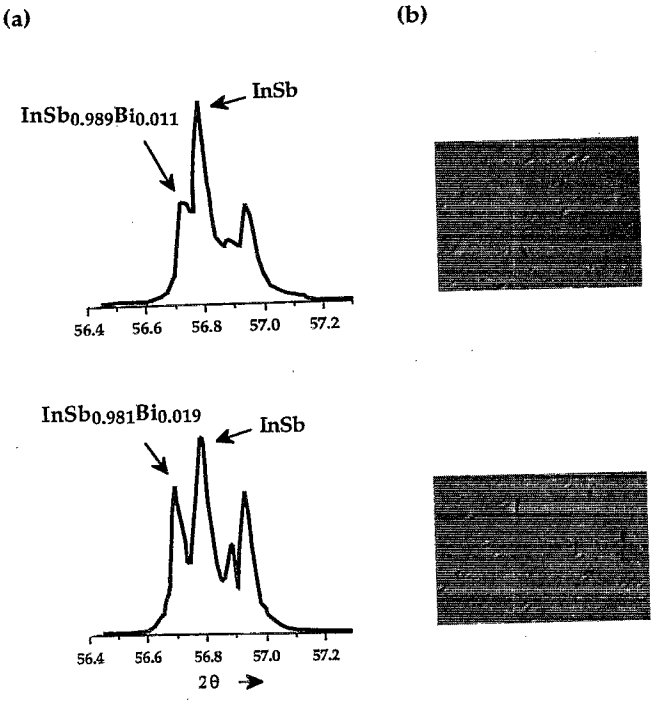

FIG. 1. (a) X-ray-diffraction scans and (b) the corresponding Nomarski interference contrast photomicrographs for $InSb_{0.0989}Bi_{0.011}$ and $InSb_{0.0981}Bi_{0.019}$ layers grown at 350 °C on InSb substrates.

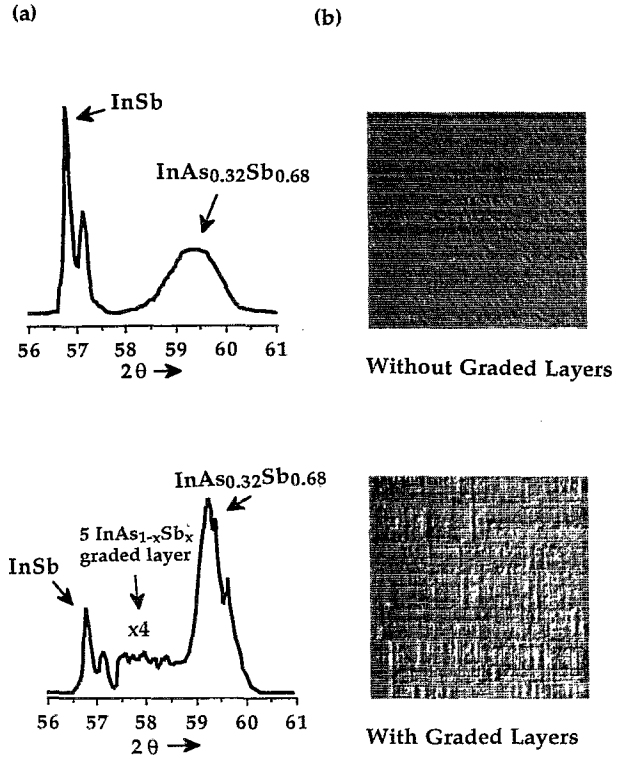

FIG. 2. Effect of the addition of step grading on (a) the x-ray scans and (b) the surface morphologies of $InAs_{0.32}Sb_{0.68}$ epilayers grown on InSb substrates.

to 0.1 eV; thus, As was added to the system. This is expected to have two effects. First, the addition of As, itself, is known to reduce the band gap of InSb. In addition, it was felt that higher Bi concentrations might be obtained, based on the much higher Bi concentrations successfully incorporated into InAs.[8] It is expected, as discussed below, that the incorporation of only 1–1.5 at. % Bi into $InAs_{0.35}Sb_{0.65}$ will be enough to reduce the 77 K energy band gap to 0.1 eV.

The growth of an InAsSbBi quaternary alloy on an InAs or an InSb substrate will generally result in a large dislocation density due to the lattice parameter mismatch. In order to minimize the deleterious effects of the lattice mismatch, we have used a compositionally step graded transition layer.[17] Each step consists of an 8 at. % Sb composition difference with a layer thickness of 0.05 μm.

Figure 2 shows the effect of the graded layer on the crystallographic quality and surface morphology of an $InAs_{0.32}Sb_{0.68}$ layer grown on an InSb substrate (2.08% lattice mismatch). Even without the step graded layer the layers have a mirrorlike, shining surface to the naked eye. However, from the x-ray-diffraction scans, a broader peak is observed from the epilayer grown without the step grading. In addition, the $K_{\alpha 1}$ and $K_{\alpha 2}$ x-ray peaks cannot be resolved for this layer. Cross-hatched surface morphologies are typically observed for the layers grown with a step-graded buffer layer. It is also possible to observe the five resolved peaks of the individual layers in the step-graded region. Including the graded layer produces epilayers with

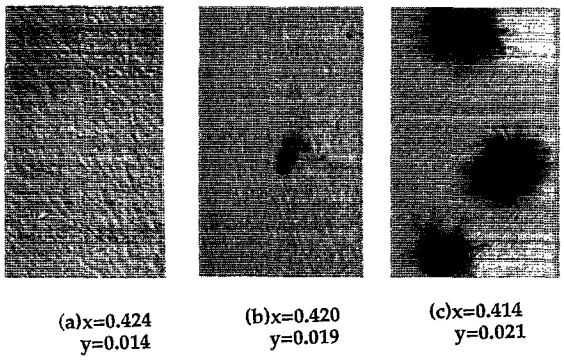

FIG. 3. Effect of Bi concentration in the solid on the surface morphologies of $InAs_{1-x-y}Sb_xBi_y$ layers with $0.41 < x < 0.43$ grown on InAs substrates.

stronger x-ray intensities and resolved $K_{\alpha 1}$ and $K_{\alpha 2}$ peaks. Thus, step grading has been used over the whole range of InAsSbBi alloys described in the remainder of this article.

Figure 3 shows the effect of increasing Bi concentration on the morphologies of $InAs_{1-x-y}Sb_xBi_y$ layers grown at 350 °C. Above a certain Bi concentration, which varies as x is changed, whiskers are formed on the surface. Scanning electron microscopy (SEM) energy-dispersive x-ray (EDAX) analysis shows that InBi is the major component in the liquid droplet at the tip of the whisker.[8] Above a certain, "optimum" Bi concentration the whiskers could not be avoided, even with a careful optimization of the growth conditions.

The variation of the Bi concentration in the solid with changing Bi/V ratio in the vapor for the growth of $InAs_{1-x-y}Sb_xBi_y$ for several values of x is shown in Fig. 4. For $x=0$, the Bi distribution coefficient K is 1.746. Since InAs is expected to be thermodynamically more stable than zinc-blende InBi, the data indicate that TMBi decomposes more rapidly than that for TBAs. Figure 4 also shows that as the value of x increases, the value of K also increases.

The growth conditions for a series of $InAs_{1-x-y}Sb_xBi_y$ layers with nearly the maximum Bi concentrations and good morphologies are summarized in Table II. Figure 5 shows the morphologies of these layers. Layers designated

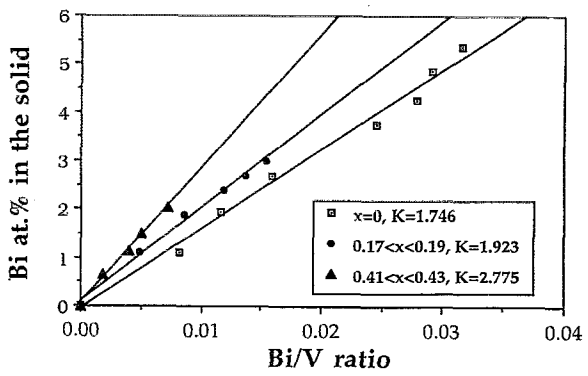

FIG. 4. The variation of Bi concentration in the solid with Bi/V ratio in the vapor for $InAs_{1-x-y}Sb_xBi_y$ ($x=0$, $0.17 < x < 0.19$, $0.41 < x < 0.43$).

TABLE II. Parameters of the OMVPE growth of $InAs_{1-x-y}Sb_xBi_y$.

Sample No.	Composition x_{Sb}[c]	Composition y_{Bi}[c]	Temperature T_g (°C)	Molar flow rate (μmol/min) EDMIn	TBAs	TBDMSb	TMBi	Input V/III ratio
IASB92[a]	0.182	0.031	350	1.131	22.990	11.242	0.538	30.749
IASB43[a]	0.310	0.027	350	1.131	22.120	22.995	0.381	40.220
IASB50[a]	0.370	0.019	350	1.131	21.876	29.481	0.291	45.660
IASB71[a]	0.420	0.020	350	1.131	14.709	31.446	0.348	41.130
IASB65[a]	0.495	0.015	350	1.131	11.315	30.817	0.226	47.460
IASB75[a]	0.591	0.014	350	1.131	5.689	31.839	0.201	33.370
IASB81[a]	0.650	0.014	350	1.131	5.917	31.997	0.162	34.670
IASB40[b]	0.852	0.013	350	1.131	2.469	32.822	0.144	31.360

[a]InAs substrate.
[b]InSb substrate.
[c]Determined by electron microprobe analysis.

(a)–(f) were grown on InAs substrates and (g) and (h) were grown on InSb substrates. Whisker-free, mirrorlike surface morphologies were observed for each layer, with a typical cross-hatched pattern observed using the Nomarski interference contrast microscope. For layers grown using the same conditions on GaAs semi-insulating substrates, even with a step-graded $InAs_{1-x}Sb_x$ buffer region, the surface morphologies had an orange-peel texture, presumably due to the extremely large lattice mismatch of $7.2\% < \Delta a/a < 14.6\%$.

The background electron carrier concentrations (77 K) for $InAs_{1-x}Sb_x$ and $InAs_{1-x-y}Sb_xBi_y$ layers grown on semi-insulating GaAs substrates at 350 °C are shown in Fig. 6. The values of y are the maximum values plotted in Fig. 7, discussed below. From comparison with the earlier data,[8] we see that replacing AsH_3 by TBAs has little effect on the background carrier concentration. The data indicate that the carrier concentration n decreases as x is increased. This is expected because the Sb—C bond strength is much lower than for the As—C bond.[18] The data also indicate that adding Bi has essentially no effect on the carrier concentration.

The relationship between the "optimum" Bi concentration y that could be incorporated into the $InAs_{1-x-y}Sb_xBi_y$ is shown as a function of the Sb content of the alloy x in Fig. 7. Nature apparently abhors small-band-gap III/V alloys. The maximum Bi content is seen to be approximately inversely related to the energy band gap as a function of x. For $InAs_{1-x}Sb_x$ alloys with $0.5 < x < 0.75$, which have the lowest-band-gap energies, the optimum Bi concentration is the lowest, 1.3–1.45 at. % for the grow temperature of 350 °C. The solid diamonds are the results of earlier work from this group[8] using traditional precursors and a higher growth temperature, since TMSb decomposes very little at temperatures below 400 °C. At 400 °C, 1.5 at. % is the highest Bi concentration obtained, even for the InAs-rich alloys. The major advance in terms of increased Bi concentration demonstrated in Fig. 7 is mainly a result of the lower growth temperature of 350 °C enabled by the use of the new Sb precursor

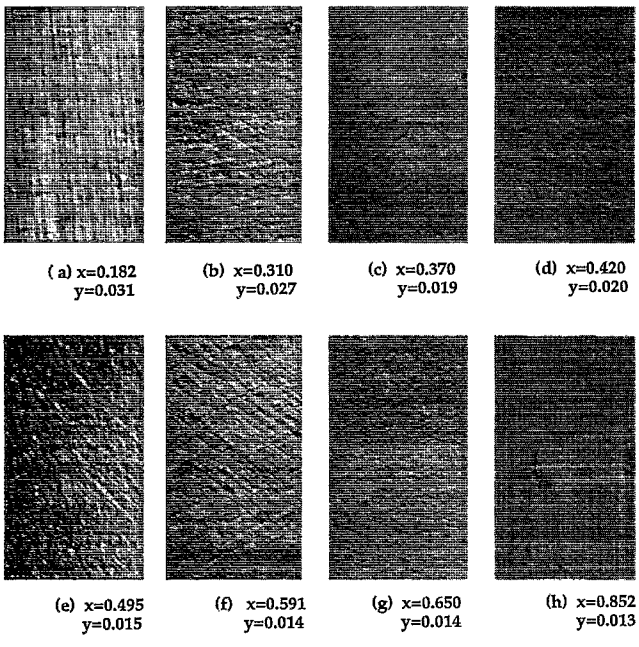

FIG. 5. Morphologies of $InAs_{1-x-y}Sb_xBi_y$ layers grown to give the highest Bi concentrations without the presence of a second phase. The substrates are InAs for (a) through (f) are InSb for (g) and (h).

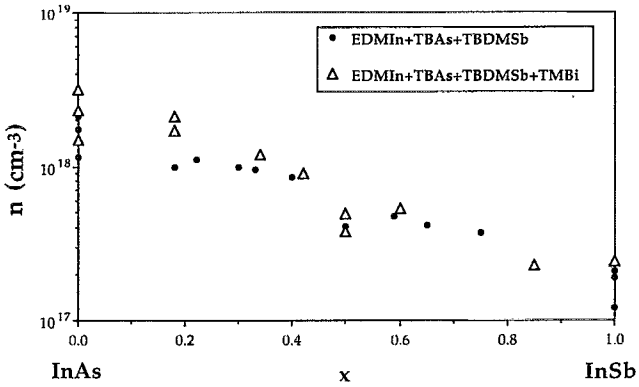

FIG. 6. Electron concentration (77 K) for $InAs_{1-x}Sb_x$ and $InAs_{1-x-y}Sb_xBi_y$ epilayers grown at 350 °C on semi-insulating GaAs substrates. The values of y are the maximum values plotted in Fig. 7.

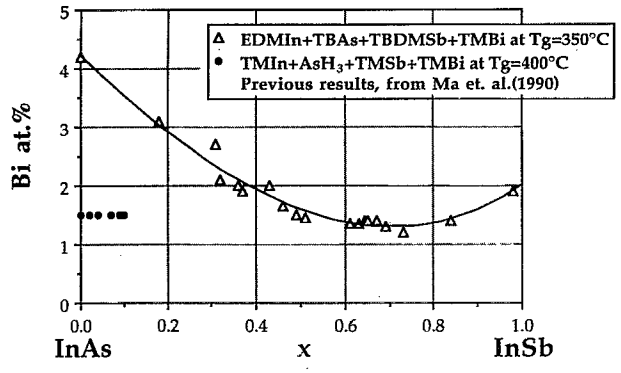

FIG. 7. Highest Bi concentration obtained without the presence of a second phase for $InAs_{1-x-y}Sb_xBi_y$ layers grown at 350 °C.

TBDMSb. The data in this figure also extend the range of Sb concentrations studied to include the entire range of $InAs_{1-x}Sb_x$ alloys.

The earlier work on $InAs_{1-x}Bi_x$ alloys showed a reduction in energy band gap with Bi concentration, dE_g/dx, of -55 meV/at. % Bi.[8] In work reported elsewhere, the range of Bi concentrations in $InAs_{1-x}Bi_x$ alloys gives PL emission was extended to 3.7 at. % Bi (Ref. 19) with the same value of dE_g/dx. Jean-Louis *et al.*[7,20] presented data indicating a value of $dE_g/dx=-36$ meV at. % Bi for $InSb_{1-x}Bi_x$ alloys. Unfortunately, the PL of the $InAs_{1-x-y}Sb_xBi_y$ layers with the maximum values of y could not be measured. One reason for this is a decrease in PL intensity as Bi is added to the solid, similar to early results for InAsBi.[8,9] Another reason is that the detection of PL at longer wavelength, even in InAsSb alloys, is difficult for the PL system used. Since the reduction of energy band gap for the addition of Bi to the InAsSb alloys has not yet been measured, we calculated the expected band-gap energies for the InAsSbBi alloys having the "optimum" Bi concentration by linearly interpolating the values of dE_g/dx between InAs and InSb, yielding $dE_g/dx=-55+19x$ (meV/% Bi). This yields the calculated values of band-gap energy for the most Bi-rich alloys having good morphologies shown in Fig. 8. Also included are the energy band gaps measured for $InAs_{1-x}Sb_x$ alloys grown as a part of this research. The results indicate that the optimum alloys for $0.3<x<0.7$ have energy band gaps of less than 0.1 eV. The smallest band-gap energy is approximately 0.08 eV. This result makes InAsSbBi alloys appear promising for IR detectors operating in the wavelength range between 8 and 12 μm.

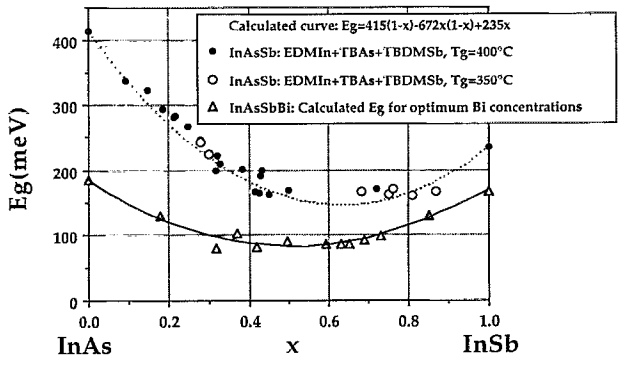

FIG. 8. Band-gap energy (10 K) vs composition for $InAs_{1-x}Sb_x$ and $InAs_{1-x-y}Sb_xBi_y$ epilayers. The broken curve is the experimental band-gap energy of $InAs_{1-x}Sb_x$ and the solid curve and triangular data points represent the band-gap energies of the $InAs_{1-x-y}Sb_xBi_y$ epilayers with the "optimum" Bi concentration.

IV. CONCLUSIONS

$InAs_{1-x-y}Sb_xBi_y$ alloys have been grown over the entire range of $0\leqslant x\leqslant 1$ by OMVPE. The use of the new precursors EDMIn, TBAs, and TBDMSb has allowed controlled growth of epitaxial layers at a substrate temperature of 350 °C. The maximum Bi concentration that can be obtained for epilayers without the presence of a second phase on the surface is found to vary dramatically from a high value of 4.5% for $x=0$ to a low of 1.5% for $x\approx 0.5$. The calculated energy band gap for $InAs_{0.485}Sb_{0.500}Bi_{0.015}$ is approximately 0.08 eV. The use of the new precursors has resulted in a major decrease in the carbon contamination of the epitaxial layers. For the alloy with the smallest band gap, the free-electron concentration is approximately 3×10^{17} cm^{-3}. These materials appear to be promising for use in the fabrication of p/n junction IR detectors operating in the 8–12 μm atmospheric window.

ACKNOWLEDGMENTS

The authors wish to thank C. H. Harmston for valuable discussions and the Office of Naval Research and the Naval Research Laboratory for supporting this work financially.

[1] G. B. Stringfellow and P. E. Greene, J. Electrochem. Soc. **118**, 805 (1971).
[2] B. F. Levine, C. G. Bethea, G. Hasnain, J. Walker, and R. J. Malik, Appl. Phys. Lett. **53**, 2196 (1988); A. Zussman, B. F. Levine, J. M. Kuo, and J. de Jong, J. Appl. Phys. **70**, 5101 (1991).
[3] M. A. Kinch and A. Yariv, Appl. Phys. Lett. **55**, 2093 (1989).
[4] I. H. Campbell, I. Sela, B. K. Laurich, D. L. Smith, C. R. Bolognesi, L. A. Samoska, A. C. Gossard, and H. Kroemer, Appl. Phys. Lett. **59**, 846 (1991); B. F. Levine, S. D. Gunapala, J. M. Kuo, S. S. Pei, and S. Hui, *ibid.* **59**, 1864 (1991); H. Xie, J. Katz, W. I. Wang, and Y. C. Chang, J. Appl. Phys. **71**, 2844 (1992).
[5] G. C. Osbourn, J. Vac. Sci. Technol. B **2**, 176 (1984).
[6] R. M. Biefeld, C. R. Hills, and S. R. Lee, J. Cryst. Growth **91**, 515 (1988).
[7] A. M. Jean-Louis and C. Hamon, Phys. Status Solidi **34**, 329 (1969).
[8] K. Y. Ma, Z. M. Fang, D. H. Jaw, R. M. Cohen, and G. B. Stringfellow, Appl. Phys. Lett. **55**, 2420 (1989); Z. M. Fang, K. Y. Ma, R. M. Cohen, and G. B. Stringfellow, J. Appl. Phys. **68**, 1187 (1990).
[9] K. Y. Ma, Z. M. Fang, R. M. Cohen, and G. B. Stringfellow, J. Cryst. Growth **107**, 416 (1991); K. Y. Ma, Z. M. Fang, R. M. Cohen, and G. B. Stringfellow, J. Appl. Phys. **68**, 4586 (1990).
[10] J. L. Zilko and J. E. Greene, J. Appl. Phys. **51**, 1549 (1980).
[11] A. J. Noreika, W. J. Takei, M. H. Francombe, and C. E. C. Wood, J. Appl. Phys. **53**, 4932 (1982).
[12] T. P. Humphreys, P. K. Chiang, S. M. Bedair, and N. R. Parikh, Appl. Phys. Lett. **53**, 142 (1988).
[13] C. A. Larsen, S. H. Li, and G. B. Stringfellow, Chem. Mater. **3**, 39 (1991).
[14] G. B. Stringfellow, J. Cryst. Growth **115**, 1 (1991).
[15] K. Y. Ma, Z. M. Fang, R. M. Cohen, and G. B. Stringfellow, J. Appl. Phys. **70**, 3940 (1991).
[16] D. S. Cao, C. H. Chen, C. W. Hill, S. H. Li, D. C. Gordon, D. W.

Brown, and B. A. Vaarstra, J. Electron. Mater. **21**, 583 (1992).
[17]D. I. Westwood and D. A. Woolf, J. Appl. Phys. **73**, 1187 (1993).
[18]S. J. W. Price, in *Comprehensive Chemical Kinetics*, edited by C. H. Bamford and C. F. H. Tipper (Elsevier, Amsterdam, 1972), Vol. 4, Sec. 2.
[19]K. T. Huang, C. T. Chiu, R. M. Cohen, and G. B. Stringfellow (unpublished results).
[20]B. Joukoff and A. M. Jean-Louis, J. Cryst. Growth **12**, 169 (1972); A. M. Jean-Louis, B. Ayrault, and J. Vargas, Phys. Status Solidi **34**, 341 (1969).